Mechanochemical Coupling of the Motion of Molecular Motors to ATP Hydrolysis

R. Dean Astumian and Martin Bier

Departments of Surgery and of Biochemistry and Molecular Biology, Section of Plastic and Reconstructive Surgery, University of Chicago, Chicago, Illinois 60637 USA

ABSTRACT The typical biochemical paradigm for coupling between hydrolysis of ATP and the performance of chemical or mechanical work involves a well-defined sequence of events (a kinetic mechanism) with a fixed stoichiometry between the number of ATP molecules hydrolyzed and the turnover of the output reaction. Recent experiments show, however, that such a deterministic picture of coupling may not be adequate to explain observed behavior of molecular motor proteins in the presence of applied forces. Here we present a general model in which the binding of ATP and release of ADP serve to modulate the binding energy of a motor protein as it travels along a biopolymer backbone. The mechanism is loosely coupled—the average number of ATPs hydrolyzed to cause a single step from one binding site to the next depends strongly on the magnitude of an applied force and on the effective viscous drag force. The statistical mechanical perspective described here offers insight into how local anisotropy along the "track" for a molecular motor, combined with an energy-releasing chemical reaction to provide a source of nonequilibrium fluctuations, can lead to macroscopic motion.

INTRODUCTION

Biological "motors" are examples of systems at the interface between the microscopic and macroscopic world. It has become possible to follow experimentally actin or microtubule movement along immobilized kinesin or myosin (Howard et al., 1989; Kuo and Scheetz, 1993) and, more recently, to follow a single kinesin molecule as it moves along a biopolymer "highway" of microtubule (Svoboda et al., 1993). It is even possible to apply an external force at a molecular level using optical tweezers and directly show that work is performed, driven by the hydrolysis of ATP. The motion of these molecular machines is dominated not by inertia and acceleration in response to a macroscopic force, but by very large viscosity and by random Brownian forces arising from collisions with the molecules of the medium. Thermal noise alone cannot of course provide the energy for powering a motor. On the other hand, the release of energy by a biochemical process such as ATP hydrolysis allows Brownian motion to be rectified (Feynman et al., 1966), resulting in net flow and work. This can in principle be accomplished by ATP hydrolysis providing a zero average fluctuating net force (Magnasco, 1993; Meister et al., 1989; Peskin et al., 1993; Vale and Oosawa, 1990) or by causing a fluctuation of the energy barriers for the diffusive process (Astumian and Bier, 1994; Peskin et al., 1994; Prost et al., 1994). The frequency response for these two mechanisms is very different (Astumian and Bier, 1994). The fluctuating force causes net flow at low frequency. With increasing frequency the flow decreases monotonically, approaching zero at very high frequency if the average force is zero. But when, with a zero net force, the heights of the barriers are caused to fluctuate, a maximum flow occurs in an intermediate frequency range and the flow vanishes at high and low frequencies. This leads to an interesting paradox. Consider diffusion on a periodic potential energy surface, where the barrier fluctuates between two states as shown in Scheme 1.

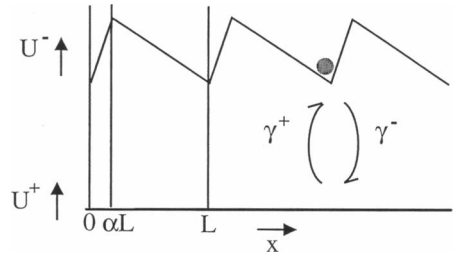

Scheme 1

$U^+(x)$ and $U^-(x)$ describe the potential energy profiles of the + and − states, respectively, transitions from U^+ to U^- and from U^- to U^+ take place at rates γ^+ and γ^-, respectively, and α defines the symmetry of the potential within a period. When the transition rates γ^+ and γ^- are very small or very large, the flux is zero. However, at intermediate frequencies the average flux is directed from left to right. It is necessary that α be smaller than ½ for the diffusion to be biased from left to right. If α is greater than ½, the diffusion is biased in the direction from right to left, as discussed by Astumian and Bier (1994). This mechanism works only by virtue of diffusion, and the ability to take energy from the nonequilibrium fluctuations is lost in the absence of thermal

Received for publication 31 March 1995 and in final form 20 October 1995.

Address reprint requests to Dr. R. Dean Astumian, Department of Surgery, University of Chicago, MC 6035, 5841 S. Maryland Ave., Chicago, IL 60637. Tel.: 312-702-6305; Fax: 312-702-1634; E-mail: dean@kramers.bsd.uchicago.edu.

0006-3495/96/02/637/00 $2.00

noise. This paradox is similar to one discussed previously in which it was shown that fluctuation of kinetic barriers for an enzyme-catalyzed process can drive the reaction thermodynamically uphill (Astumian et al., 1987, 1989; Astumian and Robertson, 1993) even if the chemical affinity is constant.

To develop a feel for this mechanism, let us consider how net flow arises. In the − state, the particle is pinned by the potential and so is localized near the bottom of a well. Immediately after a transition from the − to the + state the particle, now on a flat surface, will diffuse. This occurs by a random walk, with an equal number of steps to the left and to the right. When the state of the system undergoes a transition back to the − state, the particle is again trapped in one of the wells. If the particle has moved to the right by a distance greater than αL but less than $(1 + \alpha)L$ it feels a potential gradient leading it to the well one period to the right of the starting point; if it has moved to the left by more than $(1 - \alpha)L$ but less than $(2 - \alpha)L$ it will similarly be trapped in the well one period to the left of the starting point; if it has stayed between αL on the right and $(1 - \alpha)L$ on the left it will remain in the well from which it started. The anisotropy introduced by having the barrier at a position not equally spaced from the well to the right and left introduces a bias in the diffusion when the system is caused to fluctuate between the + and − states. If $\alpha < ½$, diffusion is biased to the right because it is more probable that the particle will diffuse a short distance αL to the right than a longer distance $(1 - \alpha)L$ to the left. If the fluctuation frequency is very low, the velocity is small because in this regime the number of "steps" (i.e., periodic displacements) per cycle $- \rightarrow + \rightarrow -$ is constant. As the frequency increases so does the velocity. At very high frequencies, however, the diffusion does not even have a chance to get started in the + state before a transition back to the pinned − state occurs and so the velocity decreases at high frequency, approaching zero as the frequency becomes infinite.

This mechanism can also serve to allow a net flow uphill, i.e., in the presence of an applied force. At some point, the applied force will be just large enough that the chance for a particle to diffuse a distance $(1 - \alpha)L$ to the left will be exactly the same as the chance to diffuse a distance αL to the right so that the velocity is zero. This is the stopping force.

How might such an asymmetric potential arise, and what could provide a mechanism for generating nonequilibrium fluctuations of an energy barrier height? Below we present a simple model in which the energy profile for a motor molecule travelling along a macromolecular highway is changed by the binding of ATP and release of ADP. As a simple example of how a potential that is periodic but locally anisotropic can arise we consider a purely electrostatic model but recognize that the situation for any actual motor must be much more complicated, involving van der Waals and hydrophobic interactions as well as conformational interactions due to the flexibility of the motor molecule. In Fig. 1 *a* we have plotted the electrostatic potential

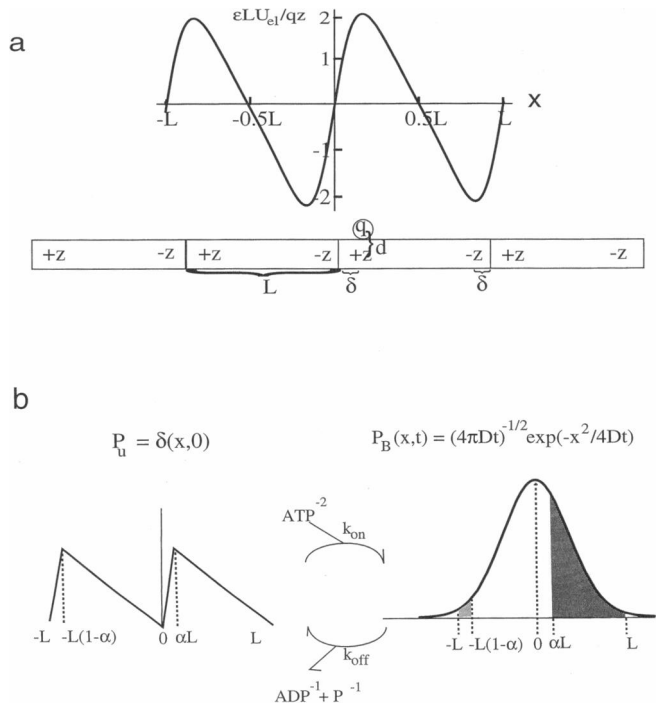

FIGURE 1 (*a*) A depiction of our model. A sphere with a charge q is diffusing on a head-to-tail linear array of dipoles (dipole moment = z [$L - 2\delta$]). The distance δ specifies how far the charges are from the end of the dipole, and the distance d specifies the charge separation when the sphere is immediately above a charge on the dipole. On top we have plotted the electric potential energy (in dimensionless units) as a function of position assuming only Coulombic interaction. The two charges on the dipole that the sphere is on as well as six charges (three dipoles) on either side were taken into account. With the dielectric constant $\epsilon = 20$, period $L = 8$ nm, $d = L/10$, $\delta = L/10$, $q = 2$ elementary charges, and $z = 3$ elementary charges, the height of the barriers relative to the wells is about 8 k_BT at $T = 300$ K. The distance between the barrier ($x = 0.15\ L$) and the well on the right ($x = 0.85\ L$) is about 0.7 L. (*b*) The behavior of a motor protein in this setup. The potential without ATP bound is treated as a piecewise linear function (for definition see text) with a barrier large enough that the probability distribution can be considered a Dirac delta function at the minimum of the potential. P_U and P_B define the probability distributions in the unbound and bound states, respectively. When ATP binds and neutralizes the charge on the Brownian particle, the potential becomes flat and the particle diffuses symmetrically. After a time interval of about $1/k_{off} = .01$ s, there is significant probability to the right of αL (the darkly shaded region), which will be caught in the well at $+L$ when ADP and P_i dissociate, but there is almost no probability to the left of $-(1 - \alpha)\ L$ (the lightly shaded region). The difference in the amount of probability on the left and right is the number of steps per ATP hydrolyzed with no applied force.

energy of a charged particle (representing kinesin) along the axis of an array of dipoles (representing tubulin monomers) aligned head to tail. For simplicity, the individual monomers are shown with all of the positive charge localized on the left-hand side and all of the negative charge localized on the right-hand side of each monomer, and the calculation of the potential energy as a function of position was done using only Coulomb's law without screening. This allows us express the potential energy in the nondimensional form shown on the graph in Fig. 1 *a*. When Debye-Huckel screening is included in the calculation for this simple case,

the relative energy difference between wells and barriers is about the same, but the potential due to the charges drops off much faster, so the wells and barriers are more localized, with a significant stretch of flat potential surface separating them. If, however, the dipole is more accurately modeled as a distribution of fixed charges given by a charge density $\rho(r')$, the electrostatic potential energy for the sphere with charge q as a function of position r is

$$U_{el}(r) = \int_{r'} \frac{q\rho(r')}{|r - r'|} \exp(-\kappa|r - r'|)\, dr'.$$

This equation explicitly includes Debye screening, where $1/\kappa$ is the Debye length of around 1–2 nm at physiological ionic strength. In this case, a potential similar both with respect to amplitude and the long-range character shown in the graph above Fig. 1 *a* is obtained for a reasonable dipole moment. As a simple explicit example, consider that the "monomer" has equally spaced charges, arranged in order from left to right, of +3, +2, +1, −1, −2, −3. Then, as the motor moves along the axis of the monomer, it is always within a Debye length of one of the charges. This gives rise to a potential similar in appearance to that calculated for the case of only two charges without screening.

If an ATP were to bind and neutralize the charge on the motor, the potential would then be almost flat. This leads us to consider the idealized model depicted in Fig. 1 *b*. In terms of Scheme 1, the transition rate from the − to + potential γ^- is k_{on} [ATP], whereas the transition rate from the + to the − potential γ^+ is k_{off}. We ignore the binding of ADP and release of ATP, which is reasonable if the ATP hydrolysis reaction is far from equilibrium.

When the barriers are up (i.e., when the motor is not bound to nucleoside phosphate) the motor is trapped in the wells and the probability density can be approximated by an array of delta functions at $-L$, 0, L, $2L$, etc. Numerically it appears that this approximation is reasonable for barriers higher than about 8 k_BT, where k_B is Boltzmann's constant and T is the Kelvin temperature. When, at $t = 0$, ATP binds, the barriers go down and the particle at $x = 0$ diffuses according to (Berg, 1983)

$$P(0|x; t) = \frac{1}{\sqrt{(4\pi Dt)}} \exp\left[\frac{-(x - (F/\beta)\, t)^2}{4Dt}\right], \quad (1)$$

where F represents an applied force, β is the coefficient of viscous friction, and D is the effective diffusion coefficient related to β through Einstein's relation $D = k_BT/\beta$. $P(0|x, t)$ is the conditional probability density that the motor is at position x at time t given that it starts at $x = 0$ at $t = 0$. The ATP remains bound for an average of $1/k_{off}$ units of time and then dissociates, causing the barriers to go back up. Motors between αL and $(\alpha + 1)L$ are caught in the well at L (i.e., one period to the right of the starting point). The probability for this is obtained by integrating the probability density Eq. 1 between these limits at the time $t = 1/k_{off}$

$$P_L = \int_{\alpha L}^{(\alpha+2)L} P(0|x; 1/k_{off})\, dx. \quad (2)$$

Similarly, the probability for the particle to be between $-(1 - \alpha)L$ and $-(2 - \alpha)L$ and thus to be caught one period to the left of the starting point, in the well at $-L$, is

$$P_{-L} = \int_{-(2-\alpha)L}^{-(1-\alpha)L} P(0|x; 1/k_{off})\, dx. \quad (3)$$

When the barrier returns to the up state by dissociation of ADP, an amount P_L will be caught in the well at $x = L$ and an amount P_{-L} will be caught in the well at $x = -L$. A net amount $P_L - P_{-L}$ is transferred to the right by one period. In a similar fashion, integrals P_{2L} and P_{-2L} can be set up for the amounts of probability ending up in the wells at $-2L$ and $2L$ and so on for $-iL$ and iL, where the limits of integration to be used are $(\alpha + i - 1)L$ to $(\alpha + i)L$, and $(-(i + 1 - \alpha)L$ to $-(i - \alpha)L$, respectively. The difference in the number of particles that end up in the well at iL and in the well at $-iL$ is $(P_{iL} - P_{-iL})$, and this contributes a net number of "steps" equal to i $(P_{iL} - P_{-iL})$. Thus R, the average number of steps of distance L per hydrolyzed ATP, equals $\Sigma_i^\infty\, i(P_{iL} - P_{-iL})$. This result can be expressed in terms of error functions, which are tabulated functions available in most packages for either symbolic or numerical algebra facilitating computation of R as a function of the various parameters. An error function results from integrating a Gaussian between limits symmetric about zero, and the complement is what is left over, i.e., twice the integral from the limit to infinity (Abramowitz and Stegun, 1970). To obtain an expression in terms of error functions, we write P_{iL}:

$$\int_{(\alpha+i-1)L}^{(\alpha+2)L} P(0|x; 1/k_{off})\, dx = \int_{(\alpha+i-1)L}^{\infty} P(0|x; 1/k_{off})\, dx - \int_{(\alpha+i)L}^{\infty} P(0|x; 1/k_{off}) dx. \quad (4)$$

A similar expression can be written for P_{-iL}. A neat feature of diffusion on a flat but tilted potential (i.e., the situation when nucleoside phosphate is bound and the motor is acted on by a homogeneous external applied force) is that the probability distribution is never distorted. Thus after a time t the probability density described by Eq. 1 is a symmetric Gaussian function even if F is not zero, but the center is at (tF/β) rather than at zero. Thus, using Eq. 1 we have

$$\int_x^\infty P(0|x'; 1/k_{off})\, dx' = \frac{1}{2}\,\mathrm{erfc}\left[\left(x - \frac{F}{\beta k_{off}}\right)\sqrt{\frac{k_{off}}{4D}}\right], \quad (5)$$

where erfc(x) is the complement of the error function (Abramowitz and Stegun, 1970). In the evaluation of the

probability for a particle to move to the left of zero, the term $F/(\beta\ k_{off})$ must be added to x in the argument of the complementary error function. The argument of the error function is dimensionless. It is useful and interesting to group the parameters in terms of ratios of characteristic time and energy scales. We define the dimensionless ratios $y = k_{off}L^2/D$ and $\varepsilon = LF/(k_BT)$. L^2/D defines the characteristic time for diffusion of a particle a distance L on a flat one-dimensional surface, and $1/k_{off}$ is the average lifetime for the "flat" (unpinned) state. LF is the energy gain (loss) when a particle is displaced by one period in the presence of an applied force F, and k_BT is the energy of the heat bath. Using Eqs. 4 and 5 and these definitions, we write

$$\sum_{i=1}^{\infty} iP_{iL} = \sum_{i=1}^{\infty} \frac{1}{2}\left\{\mathrm{erfc}\left(\frac{\sqrt{y}}{2}\left((\alpha + i - 1) - \frac{\varepsilon}{y}\right)\right) - \mathrm{erfc}\left(\frac{\sqrt{y}}{2}\left((\alpha + i) - \frac{\varepsilon}{y}\right)\right)\right\} \quad (6)$$

$$= \sum_{i=1}^{\infty} \frac{1}{2}\,\mathrm{erfc}\left(\frac{\sqrt{y}}{2}\left((\alpha + i - 1) - \frac{\varepsilon}{y}\right)\right).$$

The net number of steps R per ATP hydrolyzed can thus be expressed as

$$\sum_{i}^{\infty} i(P_{iL} - P_{-iL}) = R = \sum_{i=1}^{\infty} \frac{1}{2}\left\{\mathrm{erfc}\left(\frac{\sqrt{y}}{2}\left((\alpha + i - 1) - \frac{\varepsilon}{y}\right)\right) - \mathrm{erfc}\left(\frac{\sqrt{y}}{2}\left((i - \alpha) + \frac{\varepsilon}{y}\right)\right)\right\}. \quad (7)$$

For $y \ll 1$ and $\varepsilon = 0$, the series converges to approximately $(\frac{1}{2} - \alpha)$, whereas for $y \gtrsim 1$ the first term of the series is a very good approximation. The theoretical maximum of R is one step per two ATP's hydrolyzed because the particle diffuses to the left or to the right with equal probability but only diffusion to the right is productive. For the flux to be zero, the arguments of the two error functions in Eq. 7 must be identical. Thus we find the force necessary to stop the particle to be

$$F_{stop} = y(2\alpha - 1)\frac{k_BT}{2L}, \quad (8)$$

which is independent of ATP concentration. Multiplying R by the rate of ATP hydrolysis and by the period L we find the average velocity to be

$$\langle v\rangle = \frac{[\mathrm{ATP}]k_{on}k_{off}}{(k_{off} + [\mathrm{ATP}]k_{on})}\,\mathrm{LR}. \quad (9)$$

Note that the velocity is a Michaelis-Menten type function of the ATP concentration. The thermodynamic efficiency is calculated as follows. When the motor moves at an average speed $\langle v\rangle$ it overcomes a drag force of $\beta\langle v\rangle$, and the output power is the product $\beta\langle v\rangle^2$. In the presence of an applied force, $F\langle v\rangle$ is added to this quantity. The input power is the rate of ATP hydrolysis multiplied by the ΔG_{ATP} for ATP hydrolysis, which is around 20 k_BT under physiological conditions.

The primary purpose of this model is didactic—to illustrate the general principle that local anisotropy coupled with a source of nonequilibrium fluctuations, modeled here as the stochastic binding of ATP and release of ADP, can give rise to effectively unidirectional motion. The model emphasizes the possibility of a purely diffusion-based mechanism. The only ingredient used in the formulation of the model has been diffusion theory. The basic principles of the model have been recently investigated experimentally using a single polystyrene sphere subjected to a modulated optical trap (Faucheux et al., 1995). The scaling for velocity versus fluctuation frequency evident in the above equations holds up very well, although no attempt was made to apply a net external force in these experiments.

Let us consider whether the model can reproduce velocities and forces experimentally observed for kinesin when reasonable parameters known for kinesin are inserted. The parameters in our model are L, β, k_{off} and (k_{on}[ATP]), and α. For kinesin motion on a microtubule, L appears to be about 8 nm, both from direct observation of the stepping of kinesin (Svoboda and Block, 1994; Svoboda et al., 1993) and from measurements of the spacing of inactive kinesin bound to the microtubule (Ray et al., 1993). The potential is flat when ATP is bound in our model. This means that in the presence of saturating ATP, the motion is relatively smooth, and an estimate of the coefficient of viscous friction β can be obtained by dividing the force needed to stop the particle by the average velocity in the absence of load. In their experiments, done at saturating ATP (500 μM), Svoboda et al. (1993) measured a maximum velocity of 500 nm/s and a stopping force of 5 pN. Taking the ratio we estimate $\beta = 10^{-5}$ N s/m. Using Einstein's relation, $D = k_BT/\beta$, we find a diffusion coefficient of $D = 4 \times 10^{-16}$ m^2/s. The kinetic parameters k_{off} and k_{on}[ATP] can be obtained by measuring the rate of ATP hydrolysis by active kinesin in the presence of microtubule as a function of [ATP]. At very large [ATP], the rate is approximately k_{off}. At very low ATP, the rate is approximately k_{on} [ATP]. We use estimates for the values for these constants in the figures because definitive experimental results are not available. The parameter α reflects the asymmetry of the potential surface, which in our model depends on the strength of the dipole of a monomer of tubulin. We used $\alpha = 0.15$ as a reasonable value in line with the simple picture given in Fig. 1 *a*. In Fig. 2 *a* we have plotted the velocity versus k_{off} for $L = 8$ nm, $\alpha = 0.15$, and $D = 4 \times 10^{-16}$ m^2/s. The time it takes to diffuse over one period when the barriers are down is around L^2/D, with $L =$ 8 nm and D on the order of 10^{-16} m^2/s; this time scale is around 0.01 s. The other important time scale in the setup is $1/k_{off}$, the average time that the potential remains flat. Significant flow occurs when these two time scales are on the same order of magnitude (Fig. 2 *a*). We have also plotted the calculated velocity as a function of [ATP] with zero applied force (Fig. 2 *b*). The calculated maximum velocity

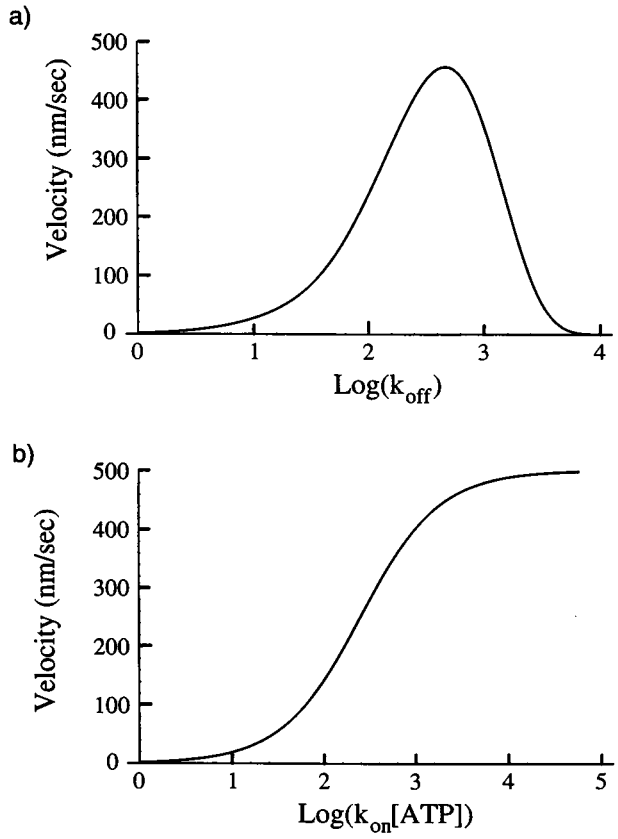

FIGURE 2 (*a*) Plot of the velocity versus $\log[k_{off}]$ as calculated from Eq. 9 with $F = 0$, $L = 8$ nm, $\beta = 10^{-5}$ N s/m (the ratio of maximum velocity to stopping force from Svoboda et al., 1993), $k_{on}[ATP] = 10^3\ s^{-1}$, and $\alpha = 0.15$. (*b*) A plot of velocity versus $\log(k_{on}[ATP])$ using $k_{off} = 250$/s and other parameters as in *a*. We checked all of our calculations against those done by solving the Fokker-Planck equation (Astumian and Bier, 1994), which does not require the approximation that the probability distribution is a delta function when the barriers are down. For energy barriers greater than 8 k_BT all numerical results were within 25% of the values obtained here.

at saturating ATP is 550 nm/s, with a stopping force of almost 5 pN. These values are consistent with the experiments of Svoboda et al. (1993).

In Fig. 3, we have plotted the velocity as a function of the force for subsaturating, half-saturating, and saturating concentrations of ATP. The stopping force is independent of ATP concentration, consistent with the recent data of Svoboda and Block (1994).

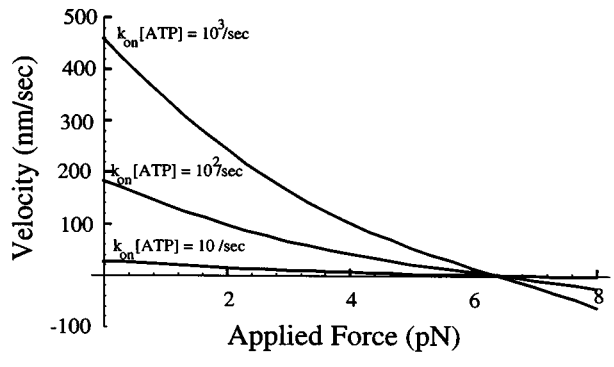

FIGURE 3 A plot of velocity versus applied force, according to Eq. 9, for saturating, half-saturating, and subsaturating ATP concentration, with all other parameter values the same as in Fig. 2 *a*.

The maximum velocity and the stopping force are not independent predictions inasmuch as we obtained the value of β used in the calculation from the ratio of the experimental maximum velocity and stopping force. Furthermore, at first glance it might seem that the value of β is unreasonably high, given known diffusion coefficients for proteins in solution that are several orders of magnitude larger than the value $D = 4 \times 10^{-16}$ m^2/s. However, even the self diffusion of ions in concentrated polyelectrolyte solutions can be much smaller than predicted, based solely on the hydrodynamic diffusion coefficient of an ion in a polyelectrolyte solution due to an effective roughening of the energy along the diffusion path—the ion must hop over many small activation barriers provided by its near neighbors (Lifson and Jackson, 1962). Furthermore, Hunt et al. (1994) have recently measured the force exerted by a single kinesin motor against a viscous load. They immobilized kinesin on a glass surface and measured the velocity of microtubules of various lengths induced by the kinesin. At low solution viscosity, the velocity was independent of the length of the microtubules. At a solution viscosity 100 times that of water, however, the velocity depended strongly on the length of the microtubules. These results are consistent with the effective viscosity between the kinesin and the microtubule being the sum of an internal viscosity coefficient, $\beta_{int} = 10^{-5}$ Ns/m, intrinsic to the interaction between kinesin and microtubule, and an external viscosity, $\beta_{ext} = C_{\|}\eta l$, where $C_{\|}$ is a dimensionless drag coefficient (determined to be about 7 by Hunt et al. (1994)), η is the solution viscosity (in N s/m^2), and l is the length of the microtubule. In the experiments the velocity decreased to about half its maximum value when $\beta_{ext} = 3 \times 10^{-6}$ N s/m, which is within an order of magnitude of the value for β_{int}, determined as the ratio of stopping force to maximum velocity measured by Svoboda et al. (1993). We expect the velocity to be about half its maximum value when $\beta_{ext} = \beta_{int}$, and thus determination of the value β_{ext} for which this holds amounts to an independent measurement of the effective viscosity coefficient, and thus the theoretical values for stopping force and velocity are independent predictions from the model. We have plotted the velocity versus external viscosity in Fig. 4 *a*.

Hunt et al. (1994) also plotted the velocity versus the apparent viscous drag force, $F_{drag} = \beta_{ext}\langle v\rangle$. They assumed this to be a linear relationship and extrapolated the experimental curve to the $\langle v\rangle = 0$ axis, interpreting the intercept 4.2 + 0.5 pN (i.e., the drag force at zero velocity) as the stopping force. For our diffusion-based model the viscous drag force must approach zero when the velocity goes to zero. In Fig. 4 *b* we have plotted parametrically the velocity (which through Eq. 7 has an explicit viscosity dependence) versus $F_{drag} = (\beta_{int} + \beta_{ext})\langle v\rangle$ according to Eq. 9. Our graph shows that at viscosities below 20 μN s/m (velocities greater than 250 nm/s) the plot of drag force versus velocity is nearly linear. In the experiments of Hunt et al. (1994) at

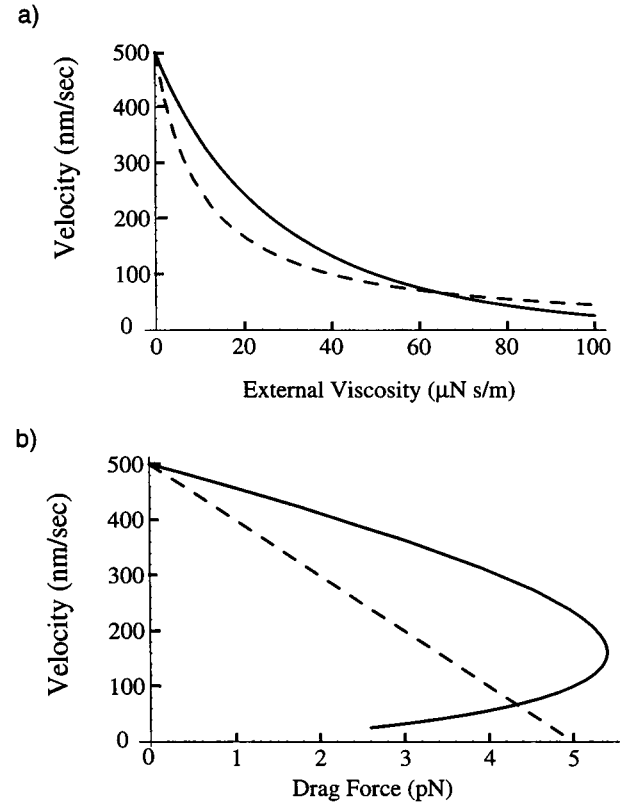

FIGURE 4 (*a*) Plot of velocity versus external viscosity, according to Eq. 9, for saturating ATP concentrations (*solid line*), with all other parameter values the same as in Fig. 2 *a*. The dashed line shows the same calculation for Scheme 2. (*b*) A parametric plot of velocity versus drag force obtained by plotting velocity versus βv for different β_{ext} according to Eq. 9 (*solid line*) and for Scheme 2 (*dashed line*).

low kinesin density, the external viscosity was at most 10 μN s/m, so their data cannot exclude our model. For very large viscosities the plot of velocity versus drag force "turns around" and moves to the origin to yield a zero drag force as the velocity goes to zero. This is because the particles never move from the bottoms of the wells, where the force due to the potential is always zero. There are other similar models, however, that are consistent with a linear plot of $\langle v \rangle$ versus $\beta_{ext}\langle v \rangle$ over a much wider range of external viscosity, such as that shown in Scheme 2 (Chauwin et al., 1994).

For simplicity, we have taken the potential in the + and − states to be identical except with a phase shift $\Delta\phi$, and we have taken the asymmetry such that $\alpha = 0$. As pointed out by Chauwin et al. (1994), this mechanism requires no diffusive steps. Each binding of ATP (with rate γ^-) and release of ADP (with rate γ^+) results in a deterministic displacement of the motor to the right resulting from the force due to the potential, which for all particles is $\Delta U/L$. What this scheme describes is a situation in which the binding site for the motor is at one position along a monomer when ATP is bound and at a different position when nucleoside phosphate is not bound. The transitions between the bound + and unbound − states occur adiabatically, and deterministic relaxation of the motor to its preferred site occurs after association of ATP or dissociation of ADP.

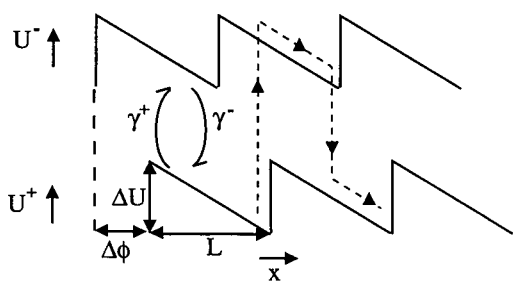

Scheme 2

The velocity of the motor sliding down the potential is $\Delta U/(\beta L)$, so the characteristic time scale for displacement by one period is $k_B TL^2/(D\Delta U)$. We have shown a typical trajectory by the dashed line for the case that the fluctuations occur slowly relative to this time scale. The displacement gets smaller as either the viscosity or the applied force is increased, but so long as the viscosity is finite and the applied force is less than $\Delta U/L$, the displacement per ATP is not zero, although the number of periods of 8 nm per ATP hydrolyzed becomes very small. Because the stopping force is 5–6 pN, we take $\Delta U = 10\, k_B T$, which when divided by $L = 8$ nm represents a force of 5 pN at room temperature. A plot of $\langle v \rangle = \Delta U/[L(\beta_{int} + \beta_{ext})]$ versus $\beta_{ext}\langle v \rangle$ is indeed linear, as shown in Fig. 4 *b* as the dashed line, where we have taken as before $\beta_{int} = 10$ μN s/m. In Fig. 4 *a*, the plot of velocity versus viscosity is shown as the dashed curve.

Schemes 1 and 2 represent limiting cases of mechanisms involving biased diffusion and "power strokes," respectively. In Scheme 1, if diffusion is very slow compared to transitions between the chemical states, the particle never moves away from a point where the potential energy is a local minimum. In the limit of very large β_{ext}, where $\langle v \rangle$ goes to zero, all of the particles feel zero force due to the potential, and hence the drag force must go to zero as well. The effect of the coefficient of viscosity appears in the exponent as well as in the pre-exponent (see Eq. 1). In Scheme 2, on the other hand, all of the particles feel the same force $F = \Delta U/L$.

Interestingly, a number of motor proteins such as dynein and the kinesin-like motor ncd move along the microtubule in the opposite direction of kinesin (MacDonald et al., 1990; Walker et al., 1990). In the model in Fig. 1, the direction of flow is reversed if the charge on the protein when ATP is not bound is zero instead of positive. A change of only a very few charged amino acids can dramatically change the behavior of the motor. The Eqs. 2 to 5 can be modified for this case by substituting $\alpha \rightarrow (1 - \alpha)$, $k_{off} \rightarrow k_{on}[\text{ATP}]$, and $k_{on}[\text{ATP}] \rightarrow k_{off}$. One prediction is that unlike the case described in Fig. 1 *b* the motor molecule will diffuse rather freely on the microtubule at low ATP concentration because the barriers are low when ATP is not bound.

Our model is phrased in terms of basic physics (electrostatic interaction and diffusion) and is very symmetric in most of its features. For the case without an applied force,

the potential energy is a periodic function of position at every instant in time, and the kinesin itself is modeled as a sphere. Even the fluctuations of the sphere's charge can be symmetric when $k_{off} = k_{on}[ATP]$. The only asymmetry is within a spatial period, where one slope is steeper than the other. The net flow is induced without any macroscopic force. In fact, in our model the role of ATP is to eliminate all local forces along the microtubule axis as well. When ATP binds, the potential is flat and the kinesin diffuses with equal probability forward and backward. The local anisotropy in the potential that arises when ATP dissociates catches the kinesin preferentially in the well to the right. If α is small, backstepping (taking a step in the "wrong" direction, i.e., right to left) is essentially precluded. In the example given with $\alpha = 0.15$, only one step backwards is predicted for every 100 steps in the forward direction. Our approach is to find in terms of basic physics (electrostatics and diffusion) the simplest and most symmetric model capable of generating the basic features of molecular motors—unidirectional motion and generation of force. This provides a fundamental theoretical basis for understanding how motor proteins may actually work in terms of experimentally determined structural features. The mechanism that we have discussed, i.e., causing flux by time-dependent shifting of kinetic barriers, is quite general and may well be important in many other biological processes, including movement of polymerase along DNA (Kabata, et al., 1993) and transport of material across membranes (Tsong and Astumian, 1986, 1988).

From the heuristic models illustrated by Fig. 1 and Schemes 1 and 2 we have learned that nonequilibrium fluctuations acting on a particle moving on an anisotropic potential can cause unidirectional motion. Furthermore, when the length and energy scales of molecular motors such as kinesin are entered into the equations resulting from consideration of these models, the calculated velocity and stopping force for the motor are consistent with what is seen experimentally. More detailed calculations show that neither model is entirely consistent with experimental fact. In particular, the viscosity dependence observed by Hunt et al. (1994) is not perfectly met by Scheme 1 and the fit coefficient of viscosity β, the stoichiometry for the number of ATP's per step, and the rate of ATP hydrolysis necessary to reproduce the experimentally determined velocities and stopping force are surprising, based on expectations from some measurements. On the other hand, in Scheme 2 we would expect that the peaks in the space correlation function (the "step" size reported by Svoboda and Block (1994)) should shift to smaller values as an applied force causes the displacement per ATP to decrease, but this is not seen experimentally.

We must remember that the two models in Schemes 1 and 2 are chosen to illustrate limiting cases for motors that strictly involve only biased Brownian motion or deterministic drift, respectively. Naturally, the actual mechanism for motion of kinesin, or any other molecular motor, most likely involves both types of motion, and it is unlikely that the potential energy as a function of the position along the microtubule is a simple "piecewise" linear function—a function that is composed of pieces, each one of which is a line—as we have used. Also, we have implicitly taken the free energy of hydrolysis of ATP to be very large in both Schemes 1 and 2. For the physiologically relevant behavior of molecular motors this is reasonable, but from a theoretical perspective it would be comforting to be able to relax the phosphorylation potential to zero and see that, as we know must be the case, the flow also goes to zero. To go further in the description of mechanochemical coupling it is necessary to treat a more general case.

A MORE GENERAL MODEL

The models described above already illustrate many of the properties of molecular motors seen experimentally. However, the analysis is valid only for the particular forms of the potential shown in Fig. 1. Furthermore, implicit in the approximations is that the ΔG_{ATP} for ATP hydrolysis is very large compared to the barrier heights. Thus we see no dependence of the velocity on ΔG_{ATP} or on the height of the barriers in the resulting equations. Next we present a more general approach. Binding rates and release rates of the nucleoside phosphates at position x_0 now may depend on the energy difference between the bound and unbound states at x_0, and the motion of the motor on each of the individual potentials is the result of the local potential gradient, of diffusion, and of any externally applied forced. The model is based on a Langevin equation:

$$\frac{dx}{dt} = \beta^{-1}\left[\frac{\partial}{\partial x} U(x, t) + F\right] + \xi(t), \tag{10}$$

Acceleration (d^2x/dt^2) does not appear in the above formulation because the mass of a molecular motor is small enough and the viscosity is large enough that the motion is damped on a time scale very short compared to any other time scale of interest. Another way of saying this is that terminal velocity after an impulse force is reached essentially instantaneously. A very lucid fundamental discussion of physics under these conditions has been given by Purcell (1977). In Eq. 10, $U(x, t)$ is the potential that undergoes transitions between the two states + and − as ATP is bound and ADP is released.

$$U^-(x) \underset{k_{off}}{\overset{k_{on}[ATP]}{\Leftrightarrow}} U^+(x), \tag{11}$$

where $U^+(x)$ is the potential function when nucleoside phosphate is bound, and $U^-(x)$ is the potential function when nucleoside phosphate is not bound to the motor. In this treatment we do not put any constraint on the shapes of $U_{free}(x)$ and $U_{bound}(x)$, except that they are periodic, because the polymer backbone (i.e., the microtubule) is periodic. F

is an external force applied, for example, by optical tweezers, and $\xi(t)$ represents Gaussian white noise with

$$\mu = \langle \xi(t) \rangle = 0; \qquad \sigma^2 = \langle \xi(t)\xi(t') \rangle = 2D\delta(t, t'). \quad (12)$$

The first of the two Eq. 12 tells us that the noise term has a zero average, and the second equation fixes the amplitude of the noise. There is a delta function in the second equation to represent the fact that we assume the noise amplitude at any time $t' = t + \Delta t$ to have no correlation to the amplitude at time t, no matter how small Δt is, i.e., the noise is taken to be "white." Equation 12 defines the statistical properties of the Gaussian noise $\xi(t)$, specified by

$$P(\xi) = \frac{1}{2\pi\sigma} \exp\left[-\frac{(\xi - \mu)^2}{2\sigma^2}\right], \quad (13)$$

which we use in simulating the Langevin Eq. 10. The delta function correlation in the expression for σ^2 indicates that in the simulation a new value of ξ must be assigned very often compared to any other time scale in the problem, in which case $\delta(t,t') \rightarrow 1$. To carry out a simulation, we take the particle at $x = 0$ when $t = 0$, and select a value for ξ from a Gaussian probability distribution Eq. 13 and an initial state ("bound" or "unbound") at random. The probability of being in the "bound" versus the "unbound" state is determined by the ratio γ^-/γ^+. The selection of the state specifies the potential function U, and ξ sets the additive force, which together determine the initial velocity of the particle. The particle moves according to Eq. 10 for a short time Δt, so the particle is somewhere other than $x = 0$. We then select a new value for ξ and give the particle a chance to change state. The probability for this change of state is given by a Poisson distribution

$$p(\text{change}) = \frac{\exp(-m)m^i}{i!},$$

where $i = t/\Delta t$ and $m = 1/(\gamma^{\pm}\Delta t)$, depending on whether the particle is in the + bound state or − unbound state. The Poisson distribution is sharply peaked about the centers $1/\gamma^{\pm}$. To meet the statistical recipe of Eq. 12 with its delta function correlation, it is necessary to choose Δt much smaller than any of the time scales $1/\gamma^+$, $1/\gamma^-$, or L^2/D. The calculation is iterated many times, keeping track of the position x of the particle at all times t.

The elements that go into the model are: 1) the two potential functions, $U^+(x)$ for when the particle is bound to ATP or ADP, and $U^-(x)$ for when the particle is not bound to a nucleoside phosphate; 2) the external force F exerted by, for example, an optical trap; 3) the coefficient of viscous friction β, which is related to the diffusion coefficient through $D = k_BT/\beta$; 4) the "white" Gaussian noise $\xi(t)$. Simulation of Eq. 10 with appropriately chosen U^-, U^+, and D (motivated by the symmetry consideration discussed in the previous section) results in a plot of x versus t (Fig. 5 *a*), which is similar to that observed experimentally (Finer et al., 1994; Svoboda and Block, 1994; Svoboda et al., 1993).

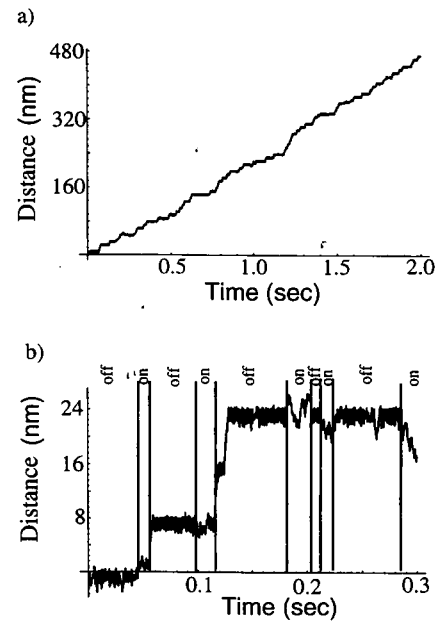

FIGURE 5 Stochastic simulation of Eq. 10 for a piecewise linear barrier of 12 k_BT in the free state and flat in the bound state, $k_{off} = 100\ s^{-1}$, k_{on} [ATP] = $100\ s^{-1}$ (with negligible reverse rates), and an asymmetry of $\alpha = 0.1$ (*b*) A close-up of a short time period within a typical simulation with $k_{off} = 50\ s^{-1}$ and k_{on} [ATP] = $10\ s^{-1}$. Note that most binding dissociation events do not lead to motion. Notice also that around $t = 0.12$ s a step occurs without hydrolysis. This just reflects the underlying noisiness of the process.

An interesting and possibly experimentally testable feature of the motion is that the amplitude in the fluctuations in position (i.e., the variance) depends on whether nucleoside phosphate is bound or not in models involving biased diffusion such as in Scheme 1, as seen in Fig. 5 *b*. When nucleoside phosphate is not bound in this model, the k_BT fluctuations can only take the particle a small distance away from the bottom of the well because the energy increases rapidly on either side of a well. On the other hand, when nucleoside phosphate is bound and the motor is in the flat + state, the potential energy does not change as the particle diffuses to the left or right and so the variance of the position caused by thermal noise is greater in this state. This difference is evident in the amplitude of the "jitter" or "jiggle" seen in Fig. 5 *b*. Thus, in principle, individual binding events can be monitored while watching an individual motor move, allowing for simultaneous determination of both velocity and ATP hydrolysis rate. The origin of the "jitter" in both the bound and unbound states is just the thermal noise acting on the system. The difference in the amplitude occurs because the k_BT energy uncertainty translates to larger noisy excursions in systems that are not constrained than in those that are energetically "stiff."

The stochastic differential Eq. 10 can be converted to a mathematically equivalent partial differential equation for the time evolution of the probability density. For a particularly elegant discussion of the equivalence of the Langevin approach and the Fokker-Planck-Smoluchowski approach

outlined below see Doi and Edwards (1986). Here we will sketch the steps leading from a continuity equation, which is very general because it is simply an expression of conservation of probability for a system, to a set of linear ordinary differential equations for the steady-state probability density as a function of position $P^{\pm}(x)$ and "state." The statistical average for any quantity of interest—the average velocity, the average "step" spacing, etc.—can be calculated from the solution $P^{\pm}(x)$, and thus comparison to experimental observation can be made. The equations of continuity for a system that can exist in two chemically distinct states are

$$\frac{\partial}{\partial t}P^{+}(x,t) = \frac{\partial}{\partial x}J^{+}(x,t) - \gamma^{+}(x)P^{+}(x,t) + \gamma^{-}(x)P^{-}(x,t)$$
$$\frac{\partial}{\partial t}P^{-}(x,t) = \frac{\partial}{\partial x}J^{-}(x,t) - \gamma^{-}(x)P^{-}(x,t) + \gamma^{+}(x)P^{+}(x,t), \quad (14)$$

where + indicates bound and − indicates free. The quantities $P^{+}(x,t)$ and $P^{-}(x,t)$ are the joint probability densities of finding the particle in the + or − state, respectively, and at position x at time t. The γ are the now possibly x-dependent rates at which transitions occur between the states from + to − (γ^{+}) and from − to + (γ^{-}). These equations represent the conservation conditions for the system. In words, they state that any change in the probability density of particles at position x and in state + (−) is due either to particles already in state + (−) flowing into or out of the infinitesimal region around x, or to a change in state of particles already at position x. For the case where inertial effects can be safely neglected, the fluxes J^{+} and J^{-} are given by

$$-J^{+} = \beta^{-1}\left(\frac{\partial U^{+}}{\partial x} + F\right)P^{+} + D\frac{\partial P^{+}}{\partial x}$$
$$-J^{-} = \beta^{-1}\left(\frac{\partial U^{-}}{\partial x} + F\right)P^{-} + D\frac{\partial P^{-}}{\partial x}. \quad (15)$$

The notation has been somewhat compressed by leaving off the explicit denotation of the functional dependence of P and U on x and t. At steady state, the time derivatives in Eq. 14 are zero, leading to two coupled ordinary differential equations for the steady-state probability distributions

$$D\frac{d^2}{dx^2}P^{+} + \frac{1}{\beta}\frac{d}{dx}\left[\left(\frac{dU^{+}}{dx} + F\right)P^{+}\right] - \gamma_{+}P^{+} + \gamma_{-}P^{-} = 0$$
$$D\frac{d^2}{dx^2}P^{-} + \frac{1}{\beta}\frac{d}{dx} + \left[\left(\frac{dU^{-}}{dx} + F\right)P^{-}\right] - \gamma_{-}P^{-} + \gamma_{+}P^{+} = 0. \quad (16)$$

These equations can be solved explicitly for "piecewise linear" potentials with constant $\gamma^{\pm}$ (Astumian and Bier, 1994). Numerical solutions for $p^{\pm}$ can be obtained for arbitrary $U^{\pm}(x)$ and $\gamma^{\pm}(x)$.

The utility of the above reaction-diffusion equation for the probability density P is that the average value of any function $f(x)$ can be calculated as $\langle f(x)\rangle = \int_0^L f(x)P(x)\,dx$. The average force on a diffusing particle then is seen to be

$$\langle\text{Force}\rangle = F + \int_0^L \left(P^{+}\frac{\partial U^{+}}{\partial x} + P^{-}\frac{\partial U^{-}}{\partial x}\right)dx. \quad (17)$$

The average velocity is related to the force through $\langle v\rangle = \langle\text{Force}\rangle/\beta$. The integral is the force that is "caused" by the fluctuations. When the integral has a larger absolute value than F and a sign opposite to that of F, we get net flow against the external force.

EQUILIBRIUM VERSUS NON-EQUILIBRIUM FLUCTUATIONS

Inevitably, the question arises as to what distinguishes equilibrium fluctuations from non-equilibrium fluctuations, and why the former can and the latter cannot give rise to net flow. Consider the following diagram:

Scheme 3

The amount of energy, $\Delta U = U^{-} - U^{+}$, necessary to change the potential from + to − depends on where the Brownian particle is along the coordinate. We will prove that if the transition rates obey the relation $\gamma^{-}/\gamma^{+} = B\exp[\Delta U/k_BT]$, where B is any constant, the flow is zero, irrespective of the properties of the potentials or the time scale of the fluctuations.

There is equilibrium if all macroscopic forces and flows vanish. In Eq. 15, this means that $F = 0$, and both J^{+} and J^{-} must individually equal zero. It is easy to verify that this is the case if $P^{\pm} = C^{\pm}\exp(-U^{\pm}/k_BT)$ where $C^{\pm}$ are arbitrary constants. By direct substitution, we see that $P^{\pm} = C^{\pm}\exp(-U^{\pm}/k_BT)$ is a solution of Eq. 17 if and only if the ratio $\gamma^{-}/\gamma^{+} = B\exp[(U^{-} - U^{+})/k_BT]$. Thus the flows $J^{\pm} = 0$ if $\gamma^{-}/\gamma^{+} = B\exp[(U^{-} - U^{+})/k_BT$, independent of $U^{\pm}(x)$ and independent of the time scale for the fluctuation.

The above relationship between γ^{+} and γ^{-} provides a necessary and sufficient condition for J^{+} and J^{-} to be individually zero. It is not necessary for this relationship to hold for the net flow $J^{+} + J^{-}$ to be zero ($J^{+} = -J^{-} \neq 0$), which occurs if both potentials U^{+} and U^{-} are isotropic (i.e., have mirror symmetry), or for the net flow to approach zero, which occurs if the fluctuations are very fast or very slow.

The issues surrounding equilibrium versus nonequilibrium noise have recently been muddied by several statements in the literature that have focused on the correlation time of the fluctuation as a key indicator of whether a

system is in equilibrium. Perhaps this is because the flow induced by fluctuations goes to zero when the fluctuation frequency becomes very large (i.e., the correlation time becomes very small) in all models if the macroscopic average force is zero. It has been suggested that "'Coloured' noise is itself a sign of a system out of equilibrium," which is simply not true. The color of noise relates to its frequency spectrum. If the spectrum is flat (featureless) at all frequencies the noise is said to be white, which is approximated by very fast fluctuations. On the other hand, if the spectrum has some features such as a drop-off at a finite frequency, the noise is said to be colored. Every chemical reaction whether at equilibrium or not gives rise to fluctuations, and the color of the fluctuations is determined by the chemical relaxation time. We have shown above that the relation $\gamma^-/\gamma^+ = B\exp[(U^- - U^+)/k_BT]$ is sufficient for all flows forces to vanish, irrespective of the individual time scales if γ^+ and γ^-. In the following we give an explicit example for a case where fluctuations are caused by a chemical reaction. We show that if the chemical reaction is at equilibrium the condition $\gamma^-/\gamma^+ = B\exp[(U^- - U^+)/k_BT$ holds and there is no flow, even though the equilibrium reaction still causes fluctuations, and these fluctuations have a finite nonzero correlation time.

One mechanism by which a non-Boltzmann distribution can be obtained is through the hydrolysis of an energy-releasing compound such as ATP. Consider the simple mechanism for ATP hydrolysis:

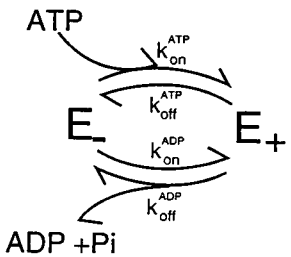

Scheme 4

where + denotes that the motor E is bound to nucleoside phosphate and − denotes that the motor is not bound to nucleoside phosphate. The hydrolysis of ATP at the active site is not explicitly shown in this standard Michaelis-Menten mechanism, but is implicit in the rate constants and their ratios, which define the overall thermodynamics of the process. From this mechanism for the ATP hydrolysis reaction, the γ are given as the sums

$$\gamma^- = k_{on}^{ATP}[ATP] + k_{on}^{ADP}[ADP];$$
$$\gamma^+ = k_{off}^{ATP} + k_{off}^{ADP}, \tag{18}$$

where $[P_i]$ is considered to be buffered and incorporated in k_{on}^{ADP}.

The ratio of the on and off rate constants for each transition must be in accord with detailed balance, i.e.,

$$\frac{k_{on}^{ATP}[ATP]}{k_{off}^{ATP}} = \exp\left[\frac{U^- - U^+}{k_BT}\right]\exp\left[\frac{\Delta G_1}{RT}\right]$$
$$\frac{k_{on}^{ADP}[ADP]}{k_{off}^{ADP}} = \exp\left[\frac{U^- - U^+}{k_BT}\right]\exp\left[\frac{\Delta G_2}{RT}\right], \tag{19}$$

where ΔG_1 and ΔG_2 are the position-independent free energy changes of binding ATP and ADP + P_i to the motor, respectively, and the U values depend on the location x. The overall thermodynamics of ATP hydrolysis is governed by the relation

$$\frac{k_{on}^{ATP}k_{off}^{ADP}[ATP]}{k_{off}^{ATP}k_{on}^{ADP}[ADP]} = \exp\left(\frac{\Delta G_{ATP}}{RT}\right), \tag{20}$$

with $\Delta G_{ATP} = \Delta G_1 - \Delta G_2$. Using Eqs. 18, 19, and 20, it is easy to show that

$$\frac{\gamma^-}{\gamma^+} = \exp\left[\frac{U^- - U^+}{k_BT}\right]\exp\left[\frac{\Delta G_2}{RT}\right] \cdot \left\{\frac{\left[\frac{k_{off}^{ATP}}{k_{off}^{ADP}}\exp\left(\frac{\Delta G_{ATP}}{RT}\right) + 1\right]}{\left[\frac{k_{off}^{ATP}}{k_{off}^{ADP}} + 1\right]}\right\}. \tag{21}$$

If $\Delta G_{ATP} = 0$ (i.e., if there is chemical equilibrium between ATP and ADP), Eq. 21 reduces to the form $\gamma^-/\gamma^+ = B\exp[(U^- - U^+)/k_BT]$. This is a sufficient condition for the flux to be zero (if $F = 0$). Furthermore, we see that if the ratio $k_{off}^{ATP}/k_{off}^{ADP}$ is independent of the position x the flow is zero even if the ΔG_{ATP} is large. What this means is that the position dependence due to $\exp(\Delta U/k_BT)$ must be expressed between the on and off rates constants differently for ATP versus ADP binding and release. The simplest case is if all of the position dependence for the ATP binding is in the "off" rate while all of the position dependence for the ADP association-dissociation is in the "on" rate. Then, far from equilibrium, only the "on" rate for ATP and "off" rate for ADP will be expressed, and the γ in Eq. 18 will be effectively position independent. Using the relations in Eq. 19, and taking k_{on}^{ATP} and k_{off}^{ADP} to be position independent, we can write the γ^+ and γ^- in terms of these rate constants as

$$\gamma^- = k_{on}^{ATP}[ATP] + k_{off}^{ADP}\exp\left(\frac{\Delta G_2}{RT}\right)\exp\left(\frac{\Delta U}{k_BT}\right);$$
$$\gamma^+ = k_{off}^{ADP} + k_{on}^{ATP}[ATP]\exp\left(\frac{-\Delta G_1}{RT}\right)\exp\left(\frac{-\Delta U}{k_BT}\right). \tag{22}$$

When $\Delta G_1 = -\Delta G_2$ (i.e., when $\Delta G_{ATP} = 0$), $\gamma^-/\gamma^+ = B\exp(\Delta U/k_BT)$, and there is no fluctuation-induced flow. However, when $\Delta G_{ATP} \gg |\Delta U/k_BT|$ for every position x, at least one of the γ is approximately position independent, and $\gamma^-/\gamma^+ \neq B\exp[(U^- - U^+)/k_BT]$.

RELATIONSHIP BETWEEN "RATCHET" MODELS AND "KINETIC" MODELS

Some earlier work on ratchet-like models for energy transduction from a fluctuating potential was motivated by consideration of the effects of fluctuation and oscillation of the membrane potential on molecular pumps—proteins in the cell and organelle membranes that use energy from ATP to do work on a concentration gradient of a substance across the membrane. As a specific example, it was shown experimentally (Serpersu and Tsong, 1984; Liu et al., 1990) that application of an oscillating electric field to a suspension of red blood cells can activate the Na^+K^+ ATPase to pump both Na^+ and K^+ from regions of low electrochemical potential to high electrochemical potential. Furthermore, the field-induced activity was independent of ATP concentration over a wide range, showing that at least part of the energy necessary for this uphill transport came from the applied field, even though the time average of the field was zero. The effect was theoretically interpreted in terms of a ratchet model (Tsong and Astumian, 1986; Astumian and Robertson, 1989; Robertson and Astumian, 1990, 1991) in which the effect of the field was to change the relative Gibbs free energies of the various states within the catalytic cycle. Surprisingly the mechanism was shown to work even if the substance transported would be electrically neutral, in which case the free-energy change through an entire cycle would be independent of the applied field and given by the difference of the chemical potentials of the transported substance on the two sides of the membrane—in other words a picture very similar to that of Scheme 1 or 2. An applied force corresponds to the difference of the electrochemical potentials, and the relative energies of the states in the catalytic cycle correspond to the details of the potential shape within a period. Based on this theoretical work, we predicted that a randomly fluctuating field would also be able to drive the transport reactions (Astumian et al., 1987, 1989). This was recently verified experimentally by Xie et al. (1994).

The theoretical work on the effects of fluctuations and oscillations of the rate constants for a chemical kinetic mechanism has much in common with more recent ratchet models involving pure diffusion (Astumian and Bier, 1994) or drift (Chauwin et al., 1994) in terms of the symmetry considerations involved. To clarify this, we have illustrated in Fig. 6, *a* and *b*, kinetic models that parallel Schemes 1 and 2, respectively. States 1 and 2 represent different positions of the motor within a period, or equivalently, different conformations of the motor protein. Each of the two states can bind both ATP and ADP, and catalyze hydrolysis, but the binding affinities depend on whether the motor is in state 1 or 2, and in turn, the relative energies of states 1 and 2 depend on whether nucleoside phosphate is or is not bound. Analogous with Schemes 1 and 2, the top curve in Fig. 6, *a* and *b*, represents the potential when nucleoside phosphate is not bound, and the bottom curve represents the potential when nucleoside phosphate is bound to the motor

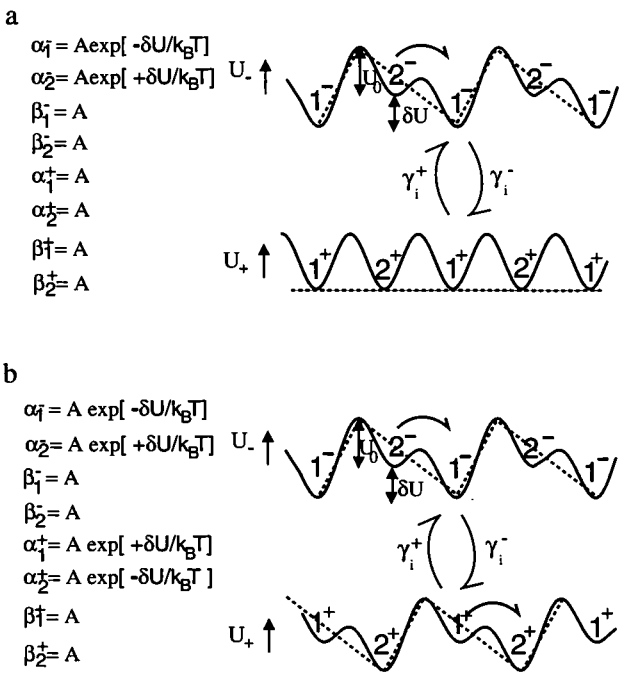

FIGURE 6 The reaction coordinates of two-state kinetic models superimposed on analogous piecewise linear ratchets (*dashed lines*). On the left are the rate constants for the different chemical transitions (discussed in text). (*a*) Flow is brought about by the anisotropic lowering and raising of activation barriers by δU as nucleoside phosphates are bound and released. The mechanism is analogous to Scheme 1. (*b*) The two-state reduction of the model of Robertson and Astumian (1990) superimposed on the piecewise linear ratchet of Chauwin et al. (1994). In this most symmetric and simplest incarnation, the top and bottom potentials are identical except for a horizontal displacement, which leads to net flow, as indicated by the curved arrows.

protein. In the kinetic picture, the binding and release of nucleoside phosphate causes the transitions $1^- \Leftrightarrow 1^+$ or $2^- \Leftrightarrow 2^+$, where each of the states 1^-, 1^+, 2^-, 2^+ are considered to be in very rapid local equilibrium, and there is no "tension" in any one of the states. Net motion is possible because the nonequilibrium fluctuations between the + and − states induced by binding, and hydrolysis of ATP and release of ADP cause a kinetic transition to the left to be more probable than a transition to the right.

The connection between a kinetic theory involving activated transitions over potential energy barriers and a diffusion theory approach based on a Fokker-Planck equation was given by Kramers (1940). For a recent review see Hanggi et al. (1990). Kramers based his approach on a separation of time scales due to the presence of barriers along a one-dimensional coordinate. The time scale for equilibration within a well is much shorter than that for equilibration between wells across the barrier if the barrier is larger than several k_BT. In this case, the rate of transition across a barrier from well i to well $i + 1$ is given by the total "concentration" in well i, n_i, multiplied by a rate constant of the form $a \exp(\Delta U_i/k_BT)$, where a is a frequency factor relating to the time scale of intra-well relaxation. For the models shown in Fig. 6, the frequency factor is $a \approx 4\ D/L^2$,

where D is the diffusion coefficient and L is the spatial period. The factor 4 appears because each well has a "length" $L/2$. In these models, the activation barriers are U_0, U_0, + δU, or U_0 − δU. Thus a factor $A = 4D \exp(U_0/k_BT)/L^2$ appears in front of each rate constant for the lateral transitions in Fig. 6, *a* and *b*. The factor $D \exp(-U_0/k_BT)$ can be thought of as an effective diffusion coefficient (Lifson and Jackson, 1962; Jackson and Coriell, 1963; Hanggi, et al., 1990) for motion of the particle along the potential. With $D = 10^{-12}$ m^2/s (the hydrodynamic diffusion coefficient for a typical protein) and $U_0 = 8\ k_BT$, $D \exp(-U_0/k_BT) = 3.3\ 10^{-16}$ m^2/s, which is in good agreement with the experimental value of Hunt et al. (1994) and with the ratio of maximum velocity and stopping force measured by Svoboda and Block (1994). This may provide a resolution to the question raised by the fact that the ratio between the stopping force and maximum velocity of a motor is much greater than the hydrodynamic coefficient of viscosity measured for motion of a typical protein through water.

Fig. 6 *a* illustrates a potential energy setup similar to that described by Astumian and Bier (1994) and Prost et al. (1994), and in the introductory part of this paper. Here, in the absence of an external field the energy is periodic in both the + and − potentials. When the nucleoside phosphate is not bound to the motor, the potential energy profile is anisotropic and the motor is tightly bound, predominantly in state 1. When nucleoside phosphate is bound the profile is more isotropic. The motors (most of which start in state 1) can execute a transition to state 2 either to the left or right with equal probability, or remain in the original state 1. When ADP dissociates, those motors that had moved to state 2 to the right now execute with high probability a transition to state 1 half a period further to the right, whereas those that had moved to state 2 to the left will predominately return to the original state. Thus there will be net flow from *left to right*, with a maximum stoichiometry of one step per two ATPs hydrolyzed. This mechanism can give rise to a maximum velocity and stopping force consistent with experiment. However, the stoichiometry necessary to obtain a velocity of 500 nm/s is greater than 5 ATPs per step with $L = 10$ nm. Thus the rate of ATP hydrolysis would have to be in excess of 250 s^{-1}.

Fig. 6 *b* is a reduction of a four-state kinetic model (Tsong and Astumian, 1986; Westerhoff et al., 1986; Astumian et al., 1987; and Robertson and Astumian; 1990), as discussed by Astumian and Robertson (1989). The analogous piecewise linear model shown as Scheme 2 and illustrated by the dashed lines in Fig. 6 *b* has been recently discussed by Chauwin et al. (1994). Here, + and − potentials work in conjunction with one another to shepherd flow from *left to right*, so this mechanism offers the possibility of a one-to-one stoichiometry. When nucleoside phosphate is bound, state 1 is energetically favored over state 2, and when the motor is not bound to nucleoside phosphate, state 2 has a lower energy than state 1. The net flow is achieved because of the asymmetry of the rate constants. In the language of chemical kinetics, we have postulated that the transition state between state 2 and state 1 to the left "looks" more like state 2, whereas the transition state between state 2 and state 1 to the right "looks" more like state 1. Because of the possibility of one-to-one stoichiometry, this model may be the most realistic possibility for the kinesin-microtubule system of the two, especially because various lines of kinetic evidence suggest that the rate of ATP hydrolysis is probably not much greater than 100 s^{-1} (Gilbert and Johnson, 1993; Huang and Hackney, 1994), presumably even while the motor is moving. Additionally, fluctuation analysis while the motor is bound to microtubule recently presented by Svoboda et al. (1994) suggests that at low load the stoichiometry is between 1 and 2 ATPs per step. The analysis of Svoboda et al. further suggests that the number of ATPs per step (i.e., the randomness) should increase with increasing load.

In general, the kinetics of the models such as those shown in Fig. 6 can be described in terms of a matrix differential equation (Astumian et al., 1989)

$$\mathrm{d}\begin{bmatrix} n_1^+ \\ n_2^+ \\ n_1^- \end{bmatrix}/\mathrm{d}t + \begin{bmatrix} (\alpha_1^+ + \beta_1^+ + \gamma_1^+) & -(\alpha_2^+ + \beta_2^+) & -\gamma_1^- \\ -(\alpha_1^+ + \beta_1^+ - \gamma_2^-) & (\alpha_2^+ + \beta_2^+ + \gamma_2^+ + \gamma_2^-) & \gamma_2^- \\ -(\gamma_1^+ - \alpha_2^- - \beta_2^-) & -(\alpha_2^- + \beta_2^-) & (\alpha_1^- + \beta_1^- + \gamma_1^- + \alpha_2^- + \beta_2^-) \end{bmatrix} \begin{bmatrix} n_1^+ \\ n_2^+ \\ n_1^- \end{bmatrix} = \begin{bmatrix} 0 \\ \gamma_2^- \\ (\alpha_2^- + \beta_2^-) \end{bmatrix}, \quad (23)$$

where we have used conservation of probability $n_2^- = 1 - n_1^+ - n_2^+ - n_1^-$. The states are given by the n, the subscript distinguishes between the lateral states 1 and 2, and the superscript distinguishes between the vertical states + and −. The α denote transition constants for a step to the right, the β denote the transition constants for a step to the left, the γ denote vertical transitions between the + and − states, and the super- and subscripts denote the originating state. Thus, β_2^+ denotes the transition constant for a step to the left starting from state n_2^+. At steady state, the time derivative is zero, and so the steady-state probabilities can be obtained explicitly by inverting the matrix of rate coefficients. The specific transition constants in terms of the potential energies of Fig. 6, *a* and *b*, are shown in the figure.

In Fig. 7 *a*, we see an alternative, equivalent way to write the mechanisms shown in Fig. 6, where now the separate transitions for ATP binding and dissociation and ADP binding and dissociation are made explicit. A similar model for coupling a redox reaction to proton flow across a membrane has been presented by Kamp et al. (1988). Movement by one period along the coordinate marked "chemistry," e.g., undergoing transition $2^- \rightarrow 2^+ \rightarrow 2^-$ from bottom to top, represents hydrolysis of one ATP, and movement by one

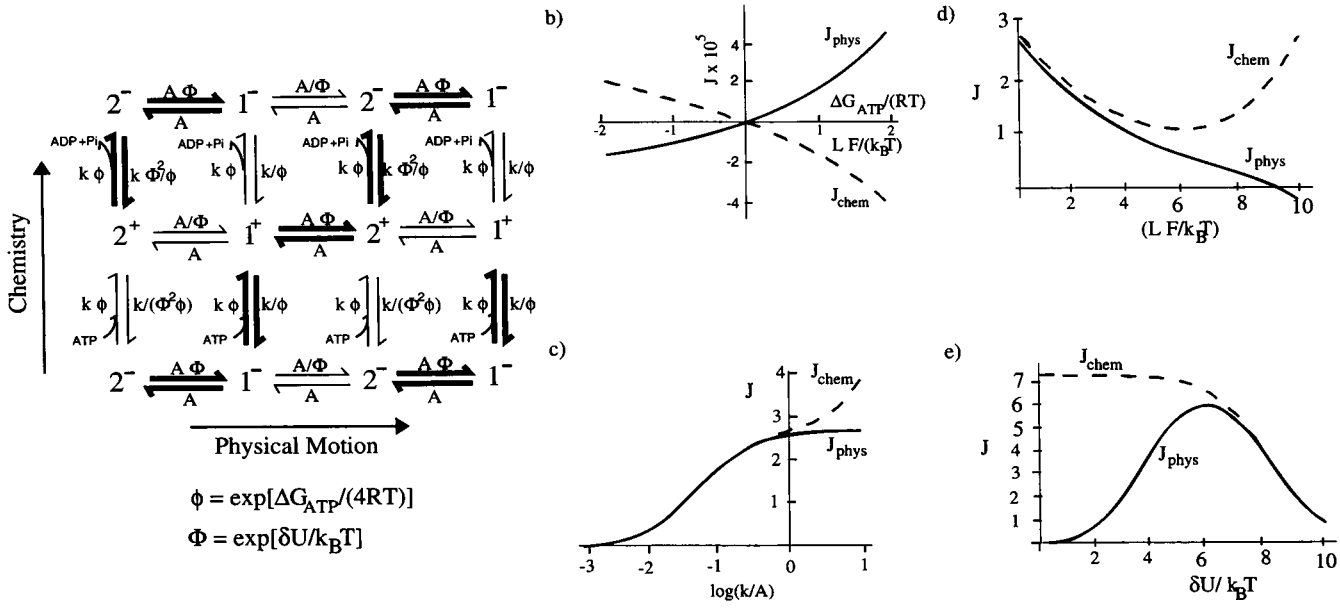

FIGURE 7 (*a*) A kinetic lattice model depicting an alternative way of writing the mechanisms of Fig. 6, *a* and *b*. The rate constants shown on the diagram are consistent with those for Fig. 6 *b*. The bold-faced transitions indicate the "coupled pathway." The steady-state probabilities are calculated from Eq. 23 with $\gamma_1^+ + \gamma_1^- = (k\phi + k/\phi)$, $\gamma_2^+ = [k\phi + k/(\Phi^2\phi)]$, and $\gamma_2^- = (k\phi + k\Phi^2/\phi)$. (*b*) Calculation of the "physical" flow J_{phys} along the *x* axis (*solid line*) induced by a small ΔG_{ATP} with $F = 0$, and the "chemical" flow J_{chem} along the *y* axis (*dashed line*) induced by a small F, with $\Delta G_{ATP} = 0$. The flow-force relations are very symmetric in this region close to equilibrium. We used $k = A = 1$ and $\delta U = 9\ k_BT$. (*c–e*) We used the standard values for the parameters $k/A = 1$, $\delta U = 9\ k_BT$, $F = 0$, $\Delta G_{ATP} = 20\ RT$ in *c*, *d*, and *e*, except that we varied one parameter in each graph, keeping the others constant. (*c*) A plot of J_{chem} and J_{phys} versus the ratio of the chemical and physical time scales, *k* and *A*, respectively. When the chemical time scale is slow compared to the physical time scale, the coupling is very tight, but as the chemical time scale becomes large compared to that for physical motion, the rate of hydrolysis continues to increase even though the rate of physical motion levels off. Thus the coupling ratio decreases. (*d*) Plot of J_{phys} and J_{chem} versus an applied external force *F*. At intermediate values of *F*, the rate of ATP hydrolysis decreases in parallel with the rate of physical motion of the motor. At large values of *F*, the rate of ATP hydrolysis increases, while the rate of physical motion continues to decrease. (*e*) Plot of J_{phys} and J_{chem} versus the interaction energy. For the kinetic models, this is equivalent to the asymmetry discussed in Scheme 1 and Fig. 1. At small δU, there is approximately no coupling between the physical and chemical processes. At intermediate δU, the coupling is strong and the flows remain appreciable. At very large δU, the coupling is essentially complete, but both chemical and physical flows become very small.

period along the coordinate marked "physical motion," e.g., undergoing transitions $2^- \rightarrow 1^- \rightarrow 2^-$ from left to right, represents displacement of the motor by one period to the right along its track. The rate constants shown on Fig. 7 *a* are consistent with the mechanism shown in Fig. 6 *b*. This way of writing the mechanism is perhaps more familiar to biochemists and stresses the coupling between physical motion, on the "*x* axis," and chemical hydrolysis of ATP, on the "*y* axis." The parametrization of the rate constants for ATP hydrolysis is by no means unique. We have taken the overall ΔG_{ATP} in the term ϕ to be equally apportioned in the four rate constants involved in ATP hydrolysis, the position dependence in the term Φ to be entirely in the "off" rate constant for ATP and the "on" rate constant for ADP, and for simplicity, we have taken the characteristic time for both ATP and ADP binding to be the same, given by *k*. The ratio of the product of forward and reverse rate constants along any path leading from a state at the bottom of the figure to the equivalent state at the top of the figure immediately above is $\exp(\Delta G_{ATP}/k_BT)$. For example, along the path $2^- \Leftrightarrow 1^- \Leftrightarrow 1^+ \Leftrightarrow 2^+ \Leftrightarrow 2^-$ going from bottom to top the ratio of forward to reverse rate constants is $(A\Phi)(k\phi)(A\Phi)(k\phi)/[(k\Phi^2/\phi)(A)(k/\phi)(A)] = \phi^4 = \exp(\Delta G_{ATP}/RT)$. In the absence of an applied force, the ratio of the products of the forward and reverse rate constants for a similar lateral displacement by a period with no vertical change is unity. If there is an applied homogeneous external force *F* (not too large), each of the left-to-right transition constants (the α) must be multiplied by $\exp[-FL/(4k_BT)]$ and each of the right-to-left transition constants (the β) must be multiplied by $\exp[+FL/(4k_BT)]$ so that the ratio of the products of forward and reverse rate constants is $\exp(F/k_BT)$. In Fig. 7 *b* we have plotted the physical flow of the motor (in periods *L* per time 1/*A*) as a function of the ΔG_{ATP} with no applied force as the solid line. The dashed line is the rate of ATP hydrolysis (ATPs per motor per unit time 1/*A*) caused by application of an external force with $\Delta G_{ATP} = 0$. The curves demonstrate the reciprocal behavior proved by Onsager (1931) for generalized coupled forces and flows—in principle, a molecular motor must be able to act as an ATP synthase at very small ΔG_{ATP}.

With the rate constants shown in Fig. 7 *a*, $\gamma_1^+ = \gamma_1^- = (k\phi + k/\phi)$, $\gamma_2^+ = [k\phi + k/(\Phi^2\phi)]$, and $\gamma_2^- = (k\phi + k\Phi^2/\phi)$, where $\phi = \exp(\Delta G_{ATP}/4k_BT)$ and $\Phi = \exp(\delta U/4k_BT)$. When ΔG_{ATP} is very large (i.e., when $\phi \gg \Phi$), all of

the γ approach $k\phi$. In this case, the transition rates between the chemical states + and − are independent of the physical position of the motor specified by state 1 or 2, which is sufficient to break detailed balance, as discussed in the section Equilibrium versus Nonequilibrium Fluctuations. The fluxes can be written in terms of the state probabilities and the rate constants. The physical flow along the ordinate can be written $J_{phys} = (A\Phi - A)\, n_1^+ + (A/\Phi - A)\, n_1^-$. Similarly, the rate of hydrolysis can be written $J_{chem} = (k\phi - k/\phi)n_1^+ + [k\phi - k/(\Phi^2\phi)]n_2^+$. In Fig. 7, *c–e*, we show how the chemical versus physical flow varies differently with changing time scale ($k\phi/A$), external force (F), and interaction energy (δU), respectively, where the standard values are taken to be $k/A = 1$, $F = 0$, and $\delta U = 9\, k_BT$. We have used units of periods L per unit time ($1/A$) for the physical flow J_{phys} to directly compare the stoichiometry between physical motion and ATP hydrolysis (J_{chem}), which is give in units of ATPs per motor per unit time ($1/A$). The stoichiometry is the ratio J_{phys}/J_{chem}. We see that the stoichiometry can indeed be close to unity under a wide range of circumstances, but this coupling is not like interlocked gears of a mechanical device. With gears, if one gear is driven so hard that the other cannot keep up, or the load is too large, the teeth of the gears may break, but it is impossible to change the coupling ratio. The coupling described by the mechanism of Fig. 7 *a* is gentler. If the viscosity of the system is changed, changing the relative time scales for physical versus chemical flow, the stoichiometry changes as seen in Fig. 7 *c*. Similarly, as an external force is applied to the motor, the system responds by changing the stoichiometry. Interestingly, a large applied force actually stimulates ATP hydrolysis, so that the rate of hydrolysis when the motor is stalled is about the same as that when there is no applied force. At intermediate forces, however, the system is still tightly coupled, and so the ATP hydrolysis initially decreases parallel with the velocity of the motor. Fig. 7 *e* illustrates the behavior as a function of interaction energy δU. At small values of δU, there is no coupling, as expected. The coupling becomes tighter as δU increases, but as δU becomes very large, both flows "shut down" and approach zero.

The coupling evident in Fig. 7 *a* is based on kinetics—thermodynamically, the transition $2^- \rightarrow 2^+$ is far more favorable than the transition $2^- \rightarrow 1^-$, with an equilibrium constant of $\phi^2\Phi^2$ for the former as compared to Φ for the latter transition. Yet, if $A\Phi > k\phi$, the transition $2^- \rightarrow 1^-$ will predominate. Is this inequality reasonable based on what we know? At large $\Delta G_{ATP} = 20k_BT$, as is the case physiologically, the rate of ATP hydrolysis is $k\phi(n_1^+ + n_2^+)$, which implies that $k\phi$ is of the order 100/s and so $k \approx$ 1/s. $A = 4\, D \exp(-U_0/k_BT)/L^2$ is about 2/s for $D = 10^{-12}$ m^2/s, $L = 10^{-8}$ m, and $U_0 = 10\, k_BT$. With $\delta U = 9\, k_BT$, $A\Phi \gg k\phi$, and at each juncture in Fig. 7 *a* the rate constant for the boldfaced transition along the coupled pathway is much greater than that for any escape transition off of the path. The pathway is set by the asymmetry, which for these kinetic models is given by δU. Even if ΔG_{ATP} were zero, the predominate flow would be along the boldfaced corridor, but the system would simply execute a random walk along this path, with no net flow in any direction. A nonzero ΔG_{ATP} is equivalent to tilting the lattice shown in Fig. 7 *a* such that the bottom is higher than the top, but where there is no tilt from left to right in the absence of an applied force F. Coupling is achieved when the lateral transitions $2^- \rightarrow 1^-$ and $1^+ \rightarrow 2^+$ are faster than the thermodynamically more favorable vertical transitions $2^- \rightarrow 2^+$ and $1^+ \rightarrow 1^-$, respectively. It might seem that the fastest coupled flow would occur when δU becomes very large, but this is not the case, as seen in Fig. 7 *e*. When δU is very large, the backward transition $2^- \rightarrow 2^+$ becomes very large compared to the forward transition $2^- \rightarrow 1^-$. Essentially, the motor becomes "stuck" in state 2^+.

Because none of the values used to obtain this condition of strong coupling are out of line with experimental values, we can conclude that the type of model proposed in Fig. 7 *a* is not inconsistent with our present knowledge of the behavior of molecular motors. Our model has predictive value in that the approach directly allows analysis of the behavior of the system under external load or at very high viscosity, as shown in Fig. 7, *c–e*. This is particularly valuable because recent advances have opened experimental approaches to carrying out such experiments at the level of a single molecule.

DISCUSSION AND CONCLUSION

Much of the work of a biological organism involves transport of material from one place to another. This includes the movement of cells and organelles by molecular motors such as kinesin and muscle, and the transport of solutes across membranes by molecular pumps such as the NaK-ATPase. Normally, we think in terms of net movement as being due to the action of macroscopic forces that provide directionality to the motion, as in the case of an object falling to the ground in the earth's gravitational field, or charged proteins electrophoresed through a gel due to an applied electric field. Molecular motors and pumps, however, effect net motion even in the absence of a macroscopic force. The energy for the movement comes typically from the hydrolysis of ATP or some other nucleoside phosphate, but it is far from clear how this chemical reaction provides a spatial gradient to define a preferred direction of motion. An emergent perspective is that a microscopic statistical mechanical point of view can offer useful insight into mechanochemical coupling.

Typically, the description of mechanoenzymes such as kinesin in muscle has involved concepts based on macroscopic ideas. These descriptions are very evocative because we all can easily relate to our own experience in the macroscopic world. Yet the picture evoked may be misleading. For example, consider the recent observation that a bead attached to a kinesin molecule has a space correlation function that is peaked at 8 nm (Svoboda and Block, 1994).

Physically, what this means is that there is a preferred spacing between locations of the bead at different times, and that a spacing of 8 nm is more likely than other spacings. It has been argued that this supports models involving "stepping" of the two kinesin heads rather than "sliding," where presumably the meaning of these words is what one would expect from a macroscopic picture. This was thought to be somewhat paradoxical because the largest dimension of the kinesin molecule is barely the size of an 8-nm period. Recent experiments have been carried out in which motion of a polystyrene particle is induced by turning on and off the modulation of an optical trap (Faucheux et al., 1995) in a manner very similar to that outlined in Scheme 1 in this paper. The space correlation function for this motion is also peaked, with a spacing given by the spatial period of the modulation of the optical trap. The physical size of the particle does not in any way determine the spacing, and because the particle is more or less spherical, moving in water, constrained by light, any description of this motion as stepping in the sense that we normally visualize stepping is not appropriate. In many instances, it seems that we should abandon classical macroscopic descriptions of the motion of motor proteins. There is no good macroscopic analogy to diffusion. The typical picture of a drunken individual undergoing a random walk is reasonable to a point, but even then we do not normally think of drunken people moving in a substance with a viscosity far greater than that of molasses—so great that the Reynold's number for the motion of the person is very small (Purcell, 1977). And yet this is the environment in which molecular motors must work.

Irreversible statistical mechanics offers an alternative to macroscopically motivated descriptions of molecular motors. A statistical mechanical description involves fundamental quantities—position, energy, and time. In such a picture, a model is specified by giving the potential energy as a function of position for each of the chemically distinct states of the motor and the transition constants (which also depend on position) for exchange between these different chemical states. The probability distribution is then calculated from the coupled Fokker-Planck-Smoluchowski equations for diffusion in the presence of local potential gradients and external forces (Eq. 16). Under certain circumstances, particularly if the potential energy functions describe several wells separated by large (>2–$3\ k_BT$) barriers within a period, the description can be simplified, taking a local equilibrium approximation within each well. This results in a kinetic description, with rate constants given by Kramers' formulae (Kramers, 1940). It is important to remember that this kinetic approach is predicated on a separation of the time scale for local equilibration within a well from the time scale for equilibration between wells. Application of strong external forces or carrying out experiments at very high viscosity can in many cases blur the distinction between these time scales. This results in a breakdown of the local equilibrium approximation, in which case a kinetic description is not appropriate.

A major advantage and disadvantage of the statistical mechanical description is that no mention whatsoever of the structure of the protein is made. All information pertaining to the structures of the proteins is compressed into the potential energy functions. This explains the surprising result that much of the behavior of an admittedly very complex and conformationally flexible molecular motor, for which the potential energy function must involve many individual interactions, can be captured by equations describing the behavior of a hard sphere moving in one dimension along a lattice of dipoles. The physical motion of any two systems that for whatever reason have identical (or sufficiently similar) reduced one-dimensional potential functions will be the same, irrespective of how complex or how simple the specific interactions giving rise to the potential functions might be.

Indeed, none of the discussion in this paper should be taken to imply that conformational change is not important in the mechanism by which molecular motors move. Almost certainly the shape of a protein changes when ATP binds, and presumably again when ATP is hydrolyzed. What seems to be important, however, and possibly experimentally distinguishable, is not so much whether this shape change occurs, but rather the character of the motion by which the change occurs. Does the conformational change occur between conformations having about the same energy, through a configurational pathway without any very large single barriers? If so, the conformational change can perhaps best be thought of as a configurational diffusion process. Or does the process occur over a large (>2–$3\ k_BT$) barrier? In which case the conformational change can perhaps be most appropriately modeled as an activated process—i.e., a chemical transformation. Or do the conformational states involved have widely different potential energies with any barriers between them smaller than this energy difference? In this case, the effect of ATP can perhaps be viewed as releasing a constraint on the system, and the resulting conformational change modeled as a classical "power stroke."

Aside from the lack of structural input, another disadvantage to models based on statistical mechanics is that it is only practical to take a one-dimensional approximation with respect to the physical coordinate. This is not an inherent weakness in the approach. The equations can easily be generalized to an arbitrary number of degrees of freedom. However, the complexity of numerical simulation of the equations increases dramatically, even with only two dimensions. Thus even such an obviously important property of kinesin as its dissociation from a microtubule cannot be practically incorporated in a description based on the Fokker-Planck-Smoluchowski equations.

Nevertheless, statistical mechanical pictures offer useful insight. The equations are derived from very fundamental physics and describe how local anisotropy along a molecular pathway, coupled with a source of nonequilibrium fluctuation, can lead to macroscopic motion in the absence of a macroscopic force. In this paper, we presented a model

for the transduction of chemical energy released by hydrolysis of ATP into mechanical energy of motion of a motor protein. The periodicity implied by the structure of microtubule and other biopolymers is a major feature of the model. For cases with no external force, the potential energy is a periodic function, and there is no net force in either the bound or the unbound state. This highlights what we consider to be the central property of molecular motors—when ATP is not bound to the motor there is no preferred direction of motion; when ATP is bound to the motor there is also no preferred direction of motion; and yet somehow the cycling between the bound and unbound states leads to unidirectional motion. We also demonstrated that the flow stops when the ATP hydrolytic reaction is at equilibrium.

The basic principles of the models have been recently tested experimentally. Rousselet et al. (1994) constructed a device similar to a standard electrophoresis apparatus along the lines suggested by Ajdari and Prost (1992), with an array of electrodes not at the ends, but along the sides. They could thus turn on and off a dielectrophoretic periodic potential without having a macroscopic force driving particles along the lane. Nevertheless, oscillation of the periodic potential caused net flow. In an even simpler system, Faucheux et al. (1995) have used an optical trap to demonstrate that time-dependent switching between periodic potential with no net force at any instant in time can still lead to unidirectional motion.

Coming from quite a different direction, the effects of oscillations and fluctuations on enzyme catalysis and particularly on membrane transport have also been studied. Recently, Xie et al. (1994) have shown that random electric pulses applied to a suspension of red blood cells can be rectified to cause unidirectional flow of ions through the NaK-ATPase. Earlier it had been shown that an externally imposed oscillation of the membrane potential acting on the NaK-ATPase is able to drive uphill transport of ions against an electrochemical gradient, even without hydrolysis of ATP (Liu, et al., 1990). The data in both cases can be fit by a four-state kinetic model similar to that of Robertson and Astumian (1990).

A major difference between recent Brownian ratchet models and more traditional tightly coupled kinetic cycle models is that ratchet models based on either diffusion or on chemical kinetics are intrinsically loosely coupled. Under certain circumstances it is possible to have an approximately constant ratio between the number of ATPs hydrolyzed and the number of steps traveled over a range of conditions, but the underlying physics does not insist on a fixed stoichiometry. Thus in the presence of an external force, the number of ATP molecules needed to cause a step is expected to increase. On the other hand, the basic picture of a cyclic kinetic model starts with the assumption of a specific sequence of steps leading to coupling between motion and hydrolysis, and only in response to experimental necessity are "slip" transitions added to the mechanism. An interesting mixture between these two pictures has been recently provided by Leibler and Huse (1993), who consider a stochastic formulation of a classical tightly coupled finite state model and treat the case of collective behavior of many motors working simultaneously.

The basic idea motivating our model is that the potential energy profile for the motor along the biopolymer track on which it moves depends on whether ATP is bound. This suggests an interesting and possibly powerful experimental test of our model. The amplitude of the fluctuations in the position of the motor must depend on the details of the potential. Thus, if the second moment of the position of the motor could be determined as a function of time (averaging for a time period long compared with the time scale of Brownian motion but short compared to the time scale of the individual steps involved in ATP hydrolysis) it should be possible to detect the individual transitions corresponding to binding and release of ATP (Funatsu et al., 1995). This would directly provide a way of determining the ATP hydrolytic rate while observing the motion of an individual motor molecule and would provide a test for distinguishing between various models.

We thank Carey Bagdassarian, Charles Doering, Marcelo Magnasco, Frank Novak, George Oster, Karel Svoboda, Ted Steck, Ed Taylor, and Tom Witten for useful discussions.

This work was supported in part by NIH grant R01ES06010.

REFERENCES

Abramowitz, M., and I. A. Stegun. 1970. Handbook of Mathematical Functions. Dover Publications, New York.

Adjari, A., and J. Prost. 1992. Mouvement induit par un potentiel de basse symétrie: dielectrophorèse pulsée. *J. C. R. Acad. Sci. Paris.* 315: 1635–1639.

Astumian, R. D., and M. Bier. 1994. Fluctuation driven ratchets: molecular motors. *Phys. Rev. Lett.* 72:1766–1769.

Astumian, R. D., P. B. Chock, T. Y. Tsong, Y.-D. Chen, and H. V. Westerhoff. 1987. Can free energy be transduced from electric noise? *Proc. Natl. Acad. Sci. USA.* 84:434–438.

Astumian, R. D., P. B. Chock, T. Y. Tsong, and H. V. Westerhoff. 1989. Effects of oscillations and energy-driven fluctuations on the dynamics of enzyme catalysis and free-energy transduction. *Phys. Rev. A.* 39: 6416–6435.

Astumian, R. D., and B. Robertson. 1989. Nonlinear effect of an oscillating electric field on membrane proteins. *J. Chem. Phys.* 91:4891–4901.

Astumian, R. D., and B. Robertson. 1993. Imposed oscillations of kinetic barriers can cause an enzyme to drive a chemical reaction away from equilibrium. *J. Am. Chem. Soc.* 115:11063–11068.

Berg, H. C. 1983. Random Walks in Biology. Princeton University Press, Princeton, NJ. 14–16, 48–51, 121–123.

Chauwin, J. F., A. Ajdari, and J. Prost. 1994. Force-free motion in asymmetric structures: a mechanism without diffusive steps. *Europhys. Lett.* 27:421–426.

Doi, M., and S. F. Edwards. 1986. The Theory of Polymer Dynamics. Oxford University Press, Oxford. Chapter 3. 46–65.

Faucheux, L. P., L. S. Bourdieu, P. D. Kaplan, and A. J. Libchaber. 1995. Optical thermal ratchets. *Phys. Rev. Lett.* 74:1504–1507.

Feynman, R. P., R. B. Leighton, and M. Sands. 1966. The Feynman Lectures on Physics, Vol. 1. Addison-Wesley, Reading, MA. Chapter 46-1–46-16.

Finer, J., R. M. Simmons, and J. A. Spudich. 1994. Single myosin molecule mechanics: piconewton forces and nanometer steps. *Nature.* 368: 113–119.

Funatsu, T., Y. Harada, M. Tokunaga, K. Saito, and T. Yanagida. 1995. Imaging of single fluorescent molecules and individual ATP turnovers by single myosin molecules in aqueous solution. *Nature.* 374:555–559.

Gilbert, S., and K. A. Johnson. 1993. Expression, purification, and characterization of the *Drosophila* kinesin motor domain produced in *Escherichia coli. Biochemistry.* 32:4677–4684.

Hanggi, P., P. Talkner, and M. Borkovec. 1990. Reaction-rate theory: fifty years after Kramers. *Rev. Mod. Phys.* 62:251–341.

Howard, J., A. J. Hudspeth, and R. D. Vale. 1989. Movement of microtubules by single kinesin molecules. *Nature.* 342:154–158.

Huang, T.-G., and D. D. Hackney. 1994. Drosophila kinesin minimal motor domain expressed in *Escherichia coli. J. Biol. Chem.* 269: 16493–16501.

Hunt, A. J., F. Gittes, and J. Howard. 1994. The force exerted by a single kinesin molecule against a viscous load. *Biophys. J.* 67:766–781.

Jackson, J. L., and S. R. Coriell. 1963. Effective diffusion constant in a polyelectrolyte solution. *J. Chem. Phys.* 38:959–968.

Kabata, H., O. Kurosawa, I. Arai, M. Washizu, S. A. Margarson, R. E. Glass, and N. Shimamoto. 1993. Visualization of single molecules of RNA polymerase sliding along DNA. *Science.* 262:1561–1563.

Kamp, F., R. D. Astumian, and H. V. Westerhoff. 1988. Coupling a biochemical reaction to proton flow down a gradient by local electric interactions. *Proc. Natl. Acad. Sci. USA.* 85:3792–3796.

Kramers, H. A. 1940. Brownian motion in a field of force and the diffusion model of chemical reactions. *Physica.* 7:284–305.

Kuo, S. C., and M. P. Sheetz. 1993. Force of single kinesin molecules measured with optical tweezers. *Science.* 260:232–234.

Leibler, S., and D. A. Huse. 1993. Porters versus rowers: a unified stochastic model of motor proteins. *J. Cell Biol.* 121:1357–1368.

Lifson, S., and J. L. Jackson. 1962. On the self diffusion of ions in a polyelectrolyte solution. *J. Chem. Phys.* 36:2410–2414.

Liu, D. S., R. D. Astumian, and T. Y. Tsong. 1990. Activation of Na^+ and K^+ pumping modes of (Na,K)-ATPase by an oscillating electric field. *J. Biol. Chem.* 265:7260–7267.

MacDonald, H. B., R. J. Stewart, and L. S. B. Goldstein. 1990. The kinesin-like *ncd* protein of Drosophila is a minus end-directed microtubule motor. *Cell.* 63:1159–1165.

Magnasco, M. 1993. Forced thermal ratchets. *Phys. Rev. Lett.* 71: 1477–1481.

Meister, M., S. R. Caplan, and H. C. Berg. 1989. Dynamics of a tightly coupled mechanism for flagellar rotation: bacterial motility, chemiosmotic coupling, protonmotive force. *Biophys. J.* 55:905–914.

Onsager, L. 1931. Reciprocal relations in irreversible processes. I. *Phys. Rev.* 37:405–425.

Peskin, C. S., B. Ermentrout, and G. Oster. 1994. The correlation ratchet: a novel mechanism for generating directed motion by ATP hydrolysis. *In* Cell Mechanics and Cellular Engineering. V. C. Mow et al., editors. Springer-Verlag, New York.

Peskin, C. S., G. M. Odell, and G. F. Oster. 1993. Cellular motions and thermal fluctuations: the Brownian ratchet. *Biophys. J.* 65:316–324.

Prost, J., J.-F. Chauwin, L. Peliti, and A. Ajdari, A. 1994. Asymmetric pumping of particles. *Phys. Rev. Lett.* 72:2652–2655.

Purcell, E. M. 1977. Life at low Reynolds number. *Am. J. Phys.* 45:3–11.

Ray, S., E. Meyhofer, R. A. Milligan, and J. Howard. 1993. Kinesin follows the microtubule's protofilament axis. *J. Cell Biol.* 121: 1083–1093.

Robertson, B., and R. D. Astumian. 1990. Michaelis-Menten equation for an enzyme in an oscillating electric field. *Biophys. J.* 58:969–974.

Robertson, B., and R. D. Astumian. 1991. Frequency dependence of catalyzed reactions in a weak oscillating field. *J. Chem. Phys.* 94: 7414–7419.

Rousselet, J., L. Salome, A. Ajdari, and J. Prost. 1994. Directional motion of Brownian particles induced by a periodic asymmetric potential. *Nature.* 370:446–448.

Serpersu, E. H., and T. Y. Tsong. 1984. Activation of electrogenic Rb^+ transport of Na,K ATPase by an electric field. *J. Biol. Chem.* 259: 7155–7162.

Svoboda, K., and S. M. Block. 1994. Force and velocity measured for single kinesin molecules. *Cell.* 77:773–784.

Svoboda, K., P. P. Mitra, and S. M. Block. 1994. Fluctuation analysis of motor protein movement and single enzyme kinetics. *Proc. Natl. Acad. Sci. USA.* 91:11782–11786.

Svoboda, K., C. F. Schmidt, B. J. Schnapp, and S. M. Block. 1993. Direct observation of kinesin stepping by optical trapping interferometry. *Nature.* 365:721–727.

Tsong, T. Y., and R. D. Astumian. 1986. Absorption and conversion of electric field energy by membrane bound ATPases. *Bioelectrochem. Bioenerg.* 15:457–476.

Tsong, T. Y., and R. D. Astumian. 1988. Electroconformational coupling: how membrane bound ATPase transduces energy from dynamic electric fields. *Annu. Rev. Physiol.* 50:273–290.

Vale, R. D., and F. Oosawa. 1990. Protein motors and Maxwell's demon: does mechanochemical transduction involve a thermal ratchet? *Adv. Biophys.* 26:97–134.

Walker, R. A., E. D. Salmon, and S. A. Endow. 1990. The *Drosophila Claret* segregation protein is a minus-end directed motor molecule. *Nature.* 347:780–782.

Westerhoff, H. V., T. Y. Tsong, P. B. Chock, Y. D. Chen, and R. D. Astumian. 1986. How an enzyme can capture free energy from an oscillating electric field. *Proc. Natl. Acad. Sci. USA.* 83:4734–4738.

Xie, T. D., P. Marszalek, Y.-D. Chen, and T. Y. Tsong. 1994. Recognition and processing of randomly fluctuating electric signals by Na,K-ATPase. *Biophys. J.* 67:1247–1251.